A Chromosome-Scale Hybrid Genome Assembly of the Extinct Tasmanian Tiger (*Thylacinus cynocephalus*)

Charles Feigin 🔟 [1,2,*], Stephen Frankenberg[1], and Andrew Pask[1,3,*]

[1]School of BioSciences, The University of Melbourne, Parkville, Victoria, Australia
[2]Department of Molecular Biology, Princeton University, New Jersey, USA
[3]Department of Sciences, Museums Victoria, Carlton, Victoria, Australia

*Corresponding authors: E-mails: charles.feigin@unimelb.edu.au; ajpask@unimelb.edu.au.

Abstract

The extinct Tasmanian tiger or thylacine (*Thylacinus cynocephalus*) was a large marsupial carnivore native to Australia. Once ranging across parts of the mainland, the species remained only on the island of Tasmania by the time of European colonization. It was driven to extinction in the early 20th century and is an emblem of native species loss in Australia. The thylacine was a striking example of convergent evolution with placental canids, with which it shared a similar skull morphology. Consequently, it has been the subject of extensive study. While the original thylacine assemblies published in 2018 enabled the first exploration of the species' genome biology, further progress is hindered by the lack of high-quality genomic resources. Here, we present a new chromosome-scale hybrid genome assembly for the thylacine, which compares favorably with many recent *de novo* marsupial genomes. In addition, we provide homology-based gene annotations, characterize the repeat content of the thylacine genome, and show that consistent with demographic decline, the species possessed a low rate of heterozygosity even compared to extant, threatened marsupials.

Key words: thylacine, Tasmanian tiger, *Thylacinus cynocephalus*, genome, Dasyuromorphia.

Significance

The lack of high-quality genomes for extinct species inhibits research into their biology. Moreover, marsupials are underrepresented among sequenced genomes. Here, we present a new, chromosome-scale thylacine genome. This high-quality assembly is a valuable new resource for studies on marsupial carnivores.

Introduction

The Tasmanian tiger or thylacine (*Thylacinus cynocephalus*; fig. 1*a*) was the largest marsupial predator of the Holocene (Mitchell et al. 2014; Prowse et al. 2014). While it once inhabited mainland Australia, by the arrival of European colonists it was restricted to the island of Tasmania (Paddle 2000; Lambeck and Chappell 2001). The thylacine was considered an agricultural pest and was targeted by an extermination campaign, incentivized by a £1 bounty (fig. 1*b*). The last known individual died in 1936 and the species was declared extinct in 1986 (Paddle 2000). The thylacine

was captured in multiple photographs and short films, contributing to its status as an emblem of Australia's high extinction rate among native species (Woinarski et al. 2015; Sleightholme and Campbell 2018).

The relative abundance of thylacine specimens in museums has facilitated the extensive study of its morphology, ecology, and evolution (Wroe et al. 2007; Newton et al. 2018; White et al. 2018; Rovinsky et al. 2021). Recently, it has also become a focal species for genomic research, with the first genome assemblies being published in 2018, using DNA from a >100-year-old ethanol-preserved

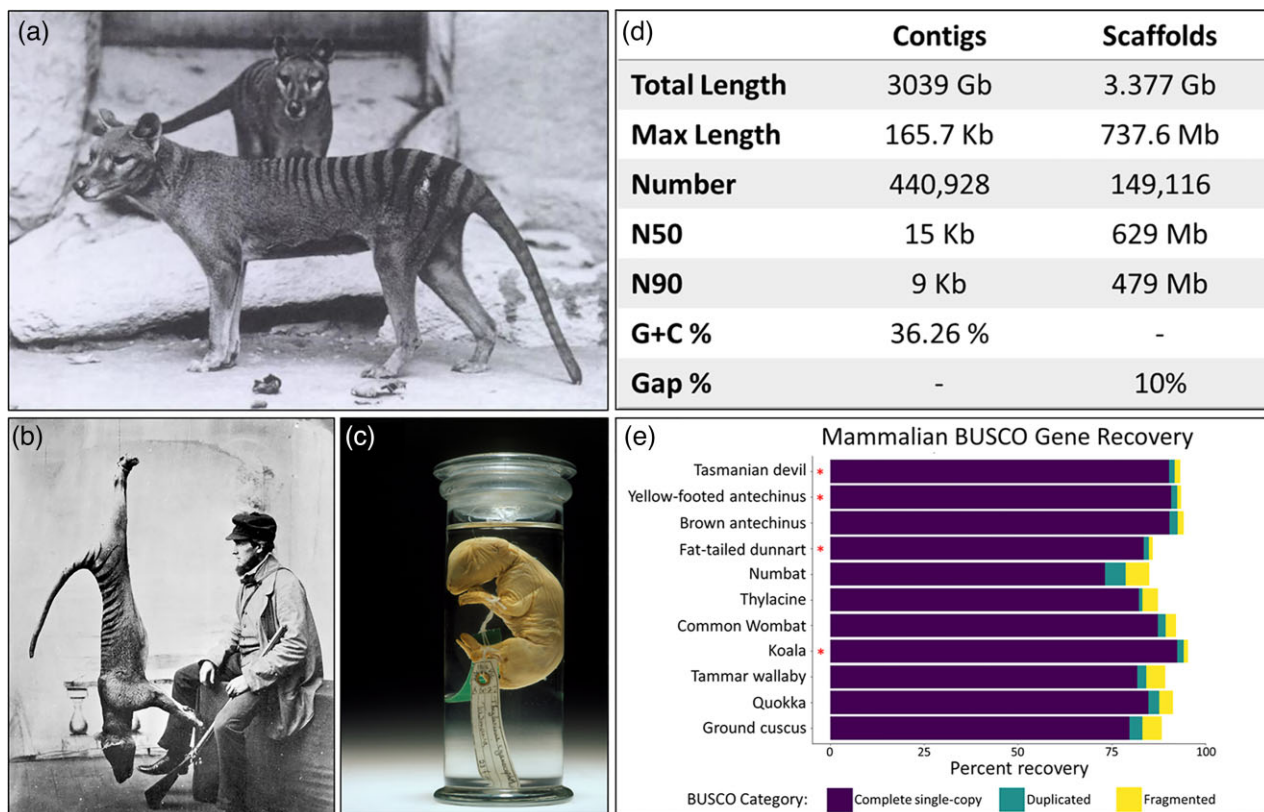| (d)	Contigs	Scaffolds
Total Length	3039 Gb	3.377 Gb
Max Length	165.7 Kb	737.6 Mb
Number	440,928	149,116
N50	15 Kb	629 Mb
N90	9 Kb	479 Mb
G+C %	36.26 %	-
Gap %	-	10%

Fig. 1.——(a) Adult thylacines in captivity. The thylacine was noted for its canid-like morphology. (b) A wild thylacine killed by a hunter. A bounty on thylacines contributed to their extinction. (c) Thylacine pouch young specimen C5757 (Melbourne Museum; Victoria, Australia) provided DNA used for genome sequencing. (d) Assembly metrics for the improved thylacine genome. (e) Comparison of the BUSCO gene recovery from the thylacine genome and several recently-released marsupial assemblies. Asterisk indicates assemblies incorporating long reads.

pouch young specimen (fig. 1c; Feigin et al. 2018). These assemblies were used to explore the molecular basis of thylacine–canid craniofacial convergence, confirm its phylogenetic relationships, and infer its demographic history (Feigin et al. 2018). Subsequent studies examined enhancer evolution and characterized the thylacine's immune gene complement (Feigin et al. 2019; Peel et al. 2021). However, the contiguity of the original assemblies was limited by the fragmentary nature of historical DNA and the absence of high-quality assemblies from related species suitable for reference-guided scaffolding (Feigin et al. 2018). This presents a substantial challenge for continued research into the thylacine's genome biology (Garrett Vieira et al. 2020; Peel et al. 2021).

The thylacine (family Thylacinidae) represents the closest sister lineage to the families Dasyuridae and Myrmecobiidae (Miller et al. 2009; Mitchell et al. 2014; Feigin et al. 2018). These groups contain numerous species of significant interest to the fields of evolutionary, developmental, and conservation biology, such as the Tasmanian devil, quolls, dunnarts, and the numbat (Fancourt 2016; Spencer et al. 2020; Wright et al. 2020; Cook et al. 2021;

Stahlke et al. 2021). Moreover, the thylacine's exceptional craniofacial similarities with canids, despite their ~160 Myr divergence, make the species an excellent model system to study the genomic basis of morphological evolution (Bininda-Emonds et al. 2007; Feigin et al. 2018; Newton et al. 2021; Rovinsky et al. 2021). Improved genomic resources for this species are thus of considerable value to the broader genomics community. Here, we leveraged improvements in short read assembly tools and newly-available marsupial reference genomes to produce a chromosome-scale hybrid genome assembly for the thylacine.

Results and Discussion

Genome Assembly and Assessment

The new thylacine assembly is composed of seven large scaffolds, corresponding to each of the six dasyuromorph autosomes and the X chromosome (supplementary table S1, Supplementary Material online), together comprising ~93.25% of the sequence content (Deakin 2018). The gap-free assembly size is ~3.04 Gbp and G + C content is

36.26%, comparable to that of the Tasmanian devil (fig. 1d and supplementary table S2, Supplementary Material online). Scaffold N50 and N90 are high (629 Mbp and 479 Mbp, respectively), reflecting the large size of dasyuromorph autosomes (Deakin 2018). Contig N50 was 5-fold higher than that of the original de novo draft assembly, and similar to that of several other recent marsupial assemblies (supplementary table S2, Supplementary Material online). A tail of small scaffolds comprising ~203.5 Mbp remained unplaced, contributing to a relatively high gap percentage (~10%; fig. 1d). Nonetheless, the new assembly represents a dramatic improvement in contiguity.

To evaluate the completeness and integrity of the assembly, BUSCO was used to annotate benchmarking mammalian orthologs. This identified 82.3% of BUSCO genes as complete and single-copy, with little duplication (0.9%). Another 4.1% were found as partial copies (fig. 1e). This is a drastic increase over the original thylacine de novo assembly, from which BUSCO recovery was negligible (<10%), owing to low contiguity (supplementary table S3, Supplementary Material online). While BUSCO gene recovery compares well with several other recently released marsupial assemblies, particularly those built from short read-based contigs scaffolded with Hi–C, it lags somewhat behind a small number of assemblies built using long reads and Hi–C (fig. 1e, supplementary table S4, Supplementary Material online). Unfortunately, the century-long room-temperature preservation of all existing thylacine tissue samples, and corresponding DNA fragmentation, limits the potential for long-read sequencing to be applied productively in this species.

Repeat Classification and Genome Annotation

Repetitive regions in the thylacine genome were annotated with RepeatMasker, using a custom database of species-specific and curated marsupial repeats (fig. 2a; Ellinghaus et al. 2008; Tarailo-Graovac and Chen 2009; Hubley et al. 2016; Flynn et al. 2020). Interspersed repeats constituted ~56% of the assembly (supplementary table S5, Supplementary Material online). Consistent with the highly conserved genome organization of dasyuromorphs, the thylacine had similar overall repeat composition to its living relatives (Tian et al. 2022). The dominant repeat class was LINE elements (~36.5%), occurring at a frequency comparable to that of the Tasmanian devil (~39%), though somewhat lower than that of the brown antechinus (~45%) (Tian et al. 2022). Interestingly, we observed that long terminal repeats were sparse in the thylacine genome (~1.51%) compared to previously studied marsupial species (which ranged from 6.53% to 18.89%; supplementary table S5, Supplementary Material online) (Tian et al. 2022).

To provide gene annotations for the new thylacine assembly, we identified orthologs to Tasmanian devil genes using a homology-based annotation liftover procedure (see Materials and Methods). Ortholog recovery was high, with ~96% of gene models being successfully transferred to the thylacine genome, comparable to or exceeding that of other dasyuromorphs (supplementary table S6, Supplementary Material online). Interestingly, we observed disparities in the detection of different short RNA classes. In particular, micro-RNAs (miRNAs) showed nearly complete recovery from the thylacine genome (~98%), compared with ~71% of small nucleolar RNAs and just ~37% of small nuclear RNAs (snoRNAs and snRNAs, respectively; supplementary table S6, Supplementary Material online). A similar pattern was observed among other dasyuromorphs, which showed lower snoRNA and snRNA recovery (particularly in species more distantly related to the Tasmanian devil), while generally retaining high miRNA recovery (supplementary table S6, Supplementary Material online). Taken together, this suggests that while many miRNAs are ancestral to Dasyuromorphia (hence having orthologs across species) and have remained conserved over time, the evolution of snRNAs and snoRNAs in this lineage has potentially been more dynamic, with accelerated sequence divergence and/or more rapid turnover of individual elements among species.

Genetic Diversity

We next sought to gain insights into the thylacine's genetic diversity prior to its extinction. Previously, multiple sequentially Markovian coalescent analysis was used to infer the demographic history of the thylacine. This uncovered evidence of an extended period of genetic decline predating the arrival of humans in Australia and the thylacine's isolation in Tasmania (Schiffels and Durbin 2014; Feigin et al. 2018). A decrease in genetic diversity concomitant with such demographic decline may have left the thylacine vulnerable to inbreeding depression, reducing its fitness against the backdrop of pressures imposed by humans. To further explore this possibility, heterozygosity was calculated in nonrepetitive regions of the thylacine genome and compared to that of extant marsupials with varying conservation statuses. Consistent with reduced genetic diversity preceding its extinction, the thylacine had the lowest rate of heterozygosity among the marsupials examined, including vulnerable or endangered species (fig. 2b and supplementary table S7, Supplementary Material online).

Conclusions

The quality of the first draft thylacine assemblies limited their utility in genomic research. Gene recovery was severely impaired by low contiguity, and repetitive regions were not adequately represented (Feigin et al. 2018). By contrast,
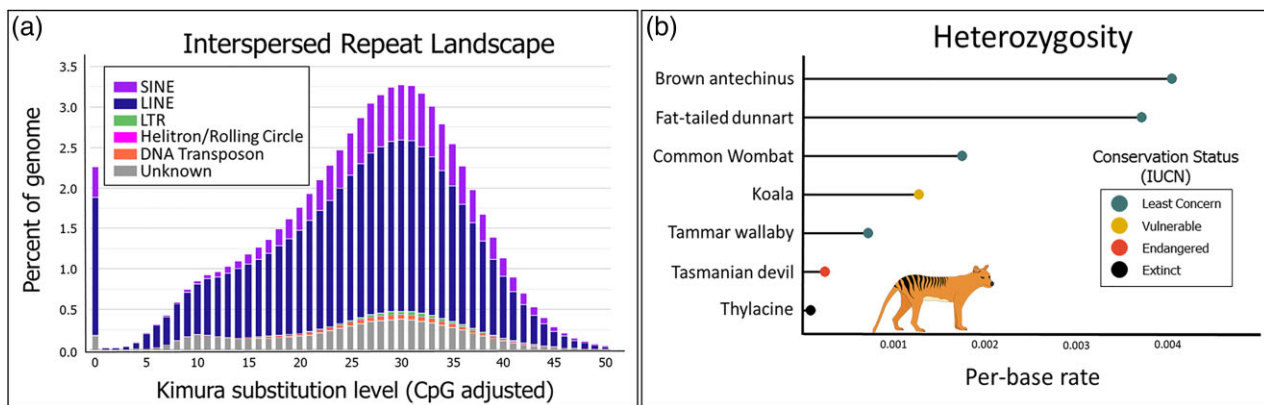
Fɪɢ. 2.——(a) Interspersed repeat landscape of the thylacine genome. The percentage of total genome size and sequence divergence (based on CpG-adjusted Kimura substitution level) are shown for each repeat subclass. (b) Comparison of the per-base rate of heterozygosity in the thylacine and several extant marsupials. The thylacine showed the lowest heterozygosity of examined marsupial species.

our new thylacine genome has a ∼5-fold larger contig N50, comparable to that of many recent marsupial assemblies. Moreover, we have produced chromosome-scale scaffolds that enable the recovery of numerous genetic elements with orthologs in related species. This assembly has also permitted the first examination of the repeat composition and heterozygosity of the thylacine genome. Future whole-genome resequencing studies, empowered by this assembly, have the potential to provide population-level insights into the thylacine's demography and level of genetic load prior to its extinction.

Materials and Methods

Genome Assembly

Thylacine reads were accessed from NCBI Sequence Read Archive (supplementary table S8, Supplementary Material online). These data originated from individual C5757, which we previously used to produce the original contig-level de novo assembly and a read-mapping-based, reference-guided assembly of non-repetitive regions (Feigin et al. 2018). Two libraries were generated using the Illumina TruSeq Nano Kit, with insert sizes of 350 and 550 bp. Both libraries were sequenced in two runs: $2 \times$ 100 bp on an Illumina HiSeq 2000 and 2×150 bp on an Illumina NextSeq 5500. Quality filtering and residual adaptor trimming were performed using Trimmomatic v0.32 with parameters: ILLUMINACLIP:2:30:10, LEADING:3 TRAILING:3 SLIDINGWINDOW:4:20 AVGQUAL20 (Feigin et al. 2018).

De novo contigs were assembled using MEGAHIT v1.2.9 (Li et al. 2015) with multiple k-mer lengths (kmers = 21, 29, 39, 59, 79, 99, 119, 141). Purging of redundant haplotypes and short read scaffolding were performed using Redundans v0.14a (parameters: identity = 0.8, overlap = 0.8, minLength = 200 bp, joins = 5, limit = 1.0, iterations = 2)

(Pryszcz and Gabaldón 2016). Purging removed ∼178.5 Mbp of sequence.

Dasyuromorphs possess an exceptionally conserved karyotype ($2n = 14$), with nearly identical chromosome sizes and g-banding patterns (Rofe and Hayman 1985; Deakin 2018). Moreover, sequence mappability between thylacine and the Tasmanian devil is high (Feigin et al. 2018). Therefore, chromosome-scale thylacine scaffolds were produced by ordering thylacine de novo scaffolds and inferring gap sizes through alignment against the recently available Tasmanian devil reference genome (GCF_902635505. 1/mSarHar1.11; O'Leary et al. 2016) using RagTag v2.1.0 (RagTag parameters: scaffold, -f 200, -r, -g 100 -m 10,000,000; minimap2 v2.22-r1101 parameters: -x asm 10) (Li 2018; Alonge et al. 2019; Alonge et al. 2021).

Genome Annotation

Repeat elements were annotated using RepeatMasker v4.1.2 (Tarailo-Graovac and Chen 2009; Flynn et al. 2020). Custom thylacine repeat libraries were produced with RepeatModeler v2.0.2a and LTRharvest v1.6.2, and were combined with marsupial repeats contained with the Dfam3.2 database (Ellinghaus et al. 2008; Hubley et al. 2016; Flynn et al. 2020). RepeatMasker was then run on each chromosome using this library (supplementary table S5, Supplementary Material online). The repeat landscape of the thylacine genome was visualized using the calcDivergenceFromAlign.pl and createRepeatLandscape.pl scripts provided with RepeatMasker. This displays the genome percentage of each repeat subclass, organized by CpG-adjusted kimura substitution level (a distance-based proxy for repeat copy age) (Kimura 1980; Flynn et al. 2020).

Given the thylacine's extinction, RNA cannot be recovered. However, annotations are essential for many genomic analyses. We, therefore, employed a homology-based

approach implemented in the program liftoff v1.6.1 to predict thylacine orthologs of Tasmanian devil genes (Shumate and Salzberg 2021). Exons from the Tasmanian devil RefSeq annotation were mapped to the thylacine genome assembly with minimap2 (O'Leary et al. 2016; Li 2018). Thylacine gene models were then produced by linking mapped exons of a common parent feature, retaining only those which preserved the structure of their corresponding Tasmanian devil reference annotation (allowing a distance factor of 4X; parameter -d 4, supplementary table S6, Supplementary Material online).

Assembly Evaluation and Comparisons

Assembly completeness and integrity were assessed using Benchmarking Universal Single-Copy Orthologs annotated by BUSCO (v5.2.2) with the mammalian_odb10 ortholog database. These results were compared with several recent *de novo* marsupial genome assemblies (fig. 1e and supplementary tables S3 and S4, Supplementary Material online) (Dudchenko et al. 2017; Johnson et al. 2018; Seppey et al. 2019; Brandies et al. 2020; Peel et al. 2022; Tian et al. 2022). Comparison genomes were chosen to represent a variety of marsupial lineages and assembly approaches released within the past 4 years. Genome assembly metrics (fig. 1d, supplementary table S2, Supplementary Material online) were calculated using the stats.sh script in the BBmap package (v37.93**)** (Bushnell 2014).

HeterozygosityTo calculate heterozygosity across species, short reads were aligned to each genome assembly with bwa-mem2 (-M flag; supplementary table S4, Supplementary Material online) (Vasimuddin et al. 2019). Samtools v1.11 was used to filter alignments (view -F 3340 -f 3) and remove duplicates (fixmate -m, markdup -r -S) (Li et al. 2009). Pileups and variant filtering were performed using bcftools v1.11 mpileup (-q 20 -Q 20 -C 50) call (-m) and view (QUAL > 20, && DP > N && DP < M, where N and M represented 0.5× and 2× the average alignment coverage post-filtering) (Danecek et al. 2021). Variants within repeats were identified with Red v2.0 and excluded using bedtools v2.27.1, due to the low accuracy of reading mapping within such regions (Quinlan and Hall 2010; Girgis 2015). This approach was applied to all genomes for this analysis rather than RepeatMasker alone, as Red has similar masking sensitivity to RepeatMasker with orders-of-magnitude lower computational overhead (Girgis 2015). Per-base heterozygosity was taken as the quotient of heterozygous positions and total callable genomic positions (fig. 2b).

Supplementary Material

Supplementary data are available at *Genome Biology and Evolution* online.

Data Availability

Thylacine data including genome assembly, gene annotations, and reads are available at NCBI BioProject PRJNA354646 and the FigShare repository at https://melbourne.figshare.com/articles/dataset/ThyCyn2_0_A_chromosome-scale_hybrid_genome_assembly_of_the_extinct_Tasmanian_tiger_Thylacinus_cynocephalus_/19351607. Dunnart reads are available at NCBI under PRJNA812859.

Literature Cited

Alonge M, et al. 2019. RaGOO: fast and accurate reference-guided scaffolding of draft genomes. Genome Biol. 20:224.

Alonge M, et al. 2021. Automated assembly scaffolding elevates a new tomato system for high-throughput genome editing. *bioRxiv*:2021.2011.2018.469135.

Bininda-Emonds OR, et al. 2007. The delayed rise of present-day mammals. Nature 446:507–512.

Brandies PA, Tang S, Johnson RSP, Hogg CJ, Belov K. 2020. The first *Antechinus* reference genome provides a resource for investigating the genetic basis of semelparity and age-related neuropathologies. Gigabyte 2020:1–22.

Bushnell B. 2014. BBMap: a fast, accurate, splice-aware aligner. Berkeley (CA): Lawrence Berkeley National Lab. (LBNL).

Cook LE, Newton AH, Hipsley CA, Pask AJ. 2021. Postnatal development in a marsupial model, the fat-tailed dunnart (*Sminthopsis crassicaudata*; Dasyuromorphia: Dasyuridae). Commun Biol. 4: 1028.

Danecek P, et al. 2021. Twelve years of SAMtools and BCFtools. GigaScience 10.

Deakin JE. 2018. Chromosome evolution in marsupials. Genes 9:72.

Dudchenko O, et al. 2017. De novo assembly of the *Aedes aegypti* genome using Hi-C yields chromosome-length scaffolds. Science 356:92–95.

Ellinghaus D, Kurtz S, Willhoeft U. 2008. LTRharvest, an efficient and flexible software for de novo detection of LTR retrotransposons. BMC Bioinform. 9:18.

Fancourt BA. 2016. Diagnosing species decline: a contextual review of threats, causes and future directions for management and conservation of the eastern quoll. Wildl Res. 43:197–211.

Feigin CY, et al. 2018. Genome of the Tasmanian tiger provides insights into the evolution and demography of an extinct marsupial carnivore. Nat Ecol Evol. 2:182–192.

Feigin CY, Newton AH, Pask AJ. 2019. Widespread cis-regulatory convergence between the extinct Tasmanian tiger and gray wolf. Genome Res. 29:1648–1658.

Flynn JM, et al. 2020. RepeatModeler2 for automated genomic discovery of transposable element families. Proc Natl Acad Sci U S A. 117: 9451–9457.

Garrett Vieira F, Samaniego Castruita JA, Gilbert MTP. 2020. Using in silico predicted ancestral genomes to improve the efficiency of paleogenome reconstruction. Ecol Evol. 10:12700–12709.

Girgis HZ. 2015. Red: an intelligent, rapid, accurate tool for detecting repeats de-novo on the genomic scale. BMC Bioinform. 16:227.

Hubley R, et al. 2016. The Dfam database of repetitive DNA families. Nucleic Acids Res. 44:D81–D89.

Johnson RN, et al. 2018. Adaptation and conservation insights from the koala genome. Nat Genet. 50:1102–1111.

Kimura M. 1980. A simple method for estimating evolutionary rates of base substitutions through comparative studies of nucleotide sequences. J Mol Evol. 16:111–120.

Lambeck K, Chappell J. 2001. Sea level change through the last glacial cycle. Science 292:679–686.

Li H, et al. 2009. The sequence alignment/map format and SAMtools. Bioinformatics 25:2078–2079.

Li H. 2018. Minimap2: pairwise alignment for nucleotide sequences. Bioinformatics 34:3094–3100.

Li D, Liu C-M, Luo R, Sadakane K, Lam T-W. 2015. MEGAHIT: an ultra-fast single-node solution for large and complex metagenomics assembly via succinct de Bruijn graph. Bioinformatics 31:1674–1676.

Miller W, et al. 2009. The mitochondrial genome sequence of the Tasmanian tiger (*Thylacinus cynocephalus*). Genome Res. 19: 213–220.

Mitchell KJ, et al. 2014. Molecular phylogeny, biogeography, and habitat preference evolution of marsupials. Mol Biol Evol. 31: 2322–2330.

Newton AH, et al. 2018. Letting the 'cat' out of the bag: pouch young development of the extinct Tasmanian tiger revealed by X-ray computed tomography. R Soc Open Sci. 5:171914.

Newton AH, Weisbecker V, Pask AJ, Hipsley CA. 2021. Ontogenetic origins of cranial convergence between the extinct marsupial thylacine and placental gray wolf. Commun Biol. 4:51.

O'Leary NA, et al. 2016. Reference sequence (RefSeq) database at NCBI: current status, taxonomic expansion, and functional annotation. Nucleic Acids Res. 44:D733–D745.

Paddle RN. 2000. The last Tasmanian tiger: the history, extinction, and myth of the thylacine. Oakleigh (VIC.): Cambridge University Press.

Peel E, et al. 2022. Genome assembly of the numbat (*Myrmecobius fasciatus*), the only termitivorous marsupial. Gigabyte 2022: 1–17.

Peel E, Frankenberg S, Hogg CJ, Pask A, Belov K. 2021. Annotation of immune genes in the extinct thylacine (*Thylacinus cynocephalus*). Immunogenetics 73:263–275.

Prowse TA, Johnson CN, Bradshaw CJ, Brook BW. 2014. An ecological regime shift resulting from disrupted predator-prey interactions in Holocene Australia. Ecology 95:693–702.

Pryszcz LP, Gabaldón T. 2016. Redundans: an assembly pipeline for highly heterozygous genomes. Nucleic Acids Res. 44:e113.

Quinlan AR, Hall IM. 2010. BEDTools: a flexible suite of utilities for comparing genomic features. Bioinformatics 26:841–842.

Rofe R, Hayman D. 1985. G-banding evidence for a conserved complement in the Marsupialia. Cytogenet Cell Genet. 39:40–50.

Rovinsky DS, Evans AR, Adams JW. 2021. Functional ecological convergence between the thylacine and small prey-focused canids. BMC Evol Biol. 21:58.

Schiffels S, Durbin R. 2014. Inferring human population size and separation history from multiple genome sequences. Nat Genet. 46: 919–925.

Seppey M, Manni M, Zdobnov EM. 2019. BUSCO: assessing genome assembly and annotation completeness. Methods Mol Biol. 1962:227–245.

Shumate A, Salzberg SL. 2021. Liftoff: accurate mapping of gene annotations. Bioinformatics 37:1639–1643.

Sleightholme SR, Campbell CR. 2018. The International Thylacine Specimen Database (6th Revision-Project Summary & Final Report). Aust Zool. 39:480–512.

Spencer PBS, McConnell S, Prada D, Friend JA. 2020. Parentage assignment using microsatellite DNA typing for the endangered numbat (*Myrmecobius fasciatus*). Aust Mammal. 42:240–243.

Stahlke AR, et al. 2021. Contemporary and historical selection in Tasmanian devils (*Sarcophilus harrisii*) support novel, polygenic response to transmissible cancer. Proc Biol Sci. 288:20210577.

Tarailo-Graovac M, Chen N. 2009. Using RepeatMasker to identify repetitive elements in genomic sequences. Curr Protoc Bioinform. Chapter 4: Unit 4.10.1–4.10.14

Tian R, et al. 2022. A chromosome-level genome of *Antechinus flavipes* provides a reference for an Australian marsupial genus with male death after mating. Mol Ecol Resour. 22:740–754.

Vasimuddin M, Misra S, Li H, Aluru S, editors. 2019. Efficient Architecture-Aware Acceleration of BWA-MEM for Multicore Systems. IEEE International Parallel and Distributed Processing Symposium (IPDPS); 2019 May 20–24; Rio de Janeiro, Brazil. IEEE. p. 314–324.

White LC, Saltré F, Bradshaw CJA, Austin JJ. 2018. High-quality fossil dates support a synchronous, Late Holocene extinction of devils and thylacines in mainland Australia. Biol Lett. 14:20170642.

Woinarski JCZ, Burbidge AA, Harrison PL. 2015. Ongoing unraveling of a continental fauna: decline and extinction of Australian mammals since European settlement. Proc Natl Acad Sci. U S A. 112: 4531–4540.

Wright BR, et al. 2020. A demonstration of conservation genomics for threatened species management. Mol Ecol Resour. 20:1526–1541.

Wroe S, Clausen P, McHenry C, Moreno K, Cunningham E. 2007. Computer simulation of feeding behaviour in the thylacine and dingo as a novel test for convergence and niche overlap. Proc Biol Sci. 274:2819–2828.

Associate editor: Bonnie Fraser